Cisplatin Inhibits Bladder Cancer Proliferation Through cGAS-STING Pathway.

GUANGHOU FU
Zhejiang University
XIAOYI CHEN
Zhejiang University School of Medicine First Affiliated Hospital
ZHIJIE XU
Zhejiang University School of Medicine First Affiliated Hospital
JUNJIE SU
Zhejiang University School of Medicine First Affiliated Hospital
JUNJIE TIAN
Zhejiang University School of Medicine First Affiliated Hospital
YUE SHI
Zhejiang University School of Medicine First Affiliated Hospital
CONGCONG XU
Zhejiang University School of Medicine First Affiliated Hospital
HAO PAN
Zhejiang University School of Medicine First Affiliated Hospital
Jin Baiye (1189006@zju.edu.cn)
Zhejiang University School of Medicine First Affiliated Hospital

Research

Keywords: Bladder cancer, Cisplatin, cGAS-STING, DNA damage, Chromatin bound

Posted Date: December 22nd, 2020

DOI: https://doi.org/10.21203/rs.3.rs-130877/v1

Abstract

Background

Cisplatin is a commonly used adjuvant chemotherapy for advanced bladder cancer, but its immune related mechanism is still unclear. Exploration the immune effects of cisplatin in bladder cancer would complement the comprehensive mechanism of cisplatin and provide the basis for combination therapy of cisplatin and immunotherapy in bladder cancer.

Methods

We confirmed the immune effects of cisplatin on T24 and TCCSUP bladder cancer cell lines in vitro and exploration the important function of these immune effects in bladder cancer microenvironment in mice tumor model.

Results

We found cisplatin induced immune response in bladder cancer by RNA sequencing, and validated cGAS-STING signal was deeply involved in this response. Cisplatin induced cGAS-STING signal inhibited the proliferation of bladder cancer and increased the infiltration percentages of CD8 + T cells and dendritic cells in transplantation mice tumor model. Accumulation of dsDNA and the release of chromatin bound cGAS are important to activate downstream STING.

Conclusion

Our findings indicated a cisplatin related immune effects in bladder cancer, cisplatin combined with immunotherapy might have a synergistic effect for bladder cancer therapy.

1. Background

1.1 Bladder cancer is one of the most common tumors in urinary system[1]. Based on pathology, bladder cancer is mainly divided into NMIBC (non-muscle invasive bladder cancer) or MIBC (muscle invasive bladder cancer), and the latter demonstrates a poorer prognosis and are recommended aggressive treatments like cystectomy combined with chemotherapy. More than 80% of bladder cancer chemotherapy is based on platinum drugs, and cisplatin is the most classic drug among them[2]. However, more than 60% of patients receiving chemotherapy strategy like neo-adjuvant chemotherapy are cisplatin resistant[3]. The critical mechanism of cisplatin resistance is still unclear. As a classical DNA cross linker, intracellular cisplatin can inhibit tumor cells by inducing irreversibility structural distortion of DNA, induce DNA damage and result in accumulated productions like dsDNA or micronucleus in tumor cells[4,5]. Over

the past decade, immunotherapy (like, PD-L1, PD1 or other) have demonstrated a promising prognostic value for MIBC therapy, and now emergent clinical trials are trying to explore the combination treatment effects of cisplatin with these new therapies. Among these clinical trials, the keynote 189 trials indicated that patients receiving platinum chemotherapy combined with PD1 showed better overall survival rates than patients receiving chemotherapy alone in non-small cell lung cancer (69.2% vs 49.4%)[6]. Cisplatin upregulated cell surface PD-L1 levels on multiple cancer types, and combination of PD-L1, PD-1 targeting therapy with cisplatin gave a synergistic effect in treating several tumor models[7–9]. The immunity function of cisplatin provides a scientific rationale to combine cisplatin with other immunotherapies.

1.2 Recently it has been reported that cGAS, an intracellular dsDNA receptor, can recognize and catalysis cytosolic dsDNA induced by cisplatin, thus activating the downstream STING signal[4]. The canonical mechanism of cGAS-STING pathway was firstly reported by Chen in 2012[10]. With further research, cGAS-STING pathway has been found to be involved in many disease processes, such as immune defense, tumor progression, autoimmune diseases, neuron degeneration[11–14]. After recognition of double-stranded DNA (dsDNA), cGAS catalyzes the cyclization of ATP and GTP into the second messenger cyclic GMP–AMP (2, 3 - cGAMP). cGAMP activate STING and result in the translocation of STING from the endoplasmic reticulum to signaling compartments, where STING enables the phosphorylation of kinase TBK1, which mediates the activation of the transcription factor interferon regulatory factor 3 (IRF3) and or nuclear factor κB (NF-κB)[4,15], and finally leads to the secretion of type interferons, like IFN-β.

1.3 The functional activity of cGAS is the critical step to activate STING pathway. Liu et al. found that the nuclear translocation of cGAS in THP-1 and HeLa cells can affect its functions by suppressing homologous-recombination-mediated repair[16]. Studies have also shown that the binding capacity of cGAS to nucleosomes is much greater than that of cGAS to dsDNA[17–21]. This can explain why the cGAS-STING signal is not significantly activated during mitosis when a large amount of dsDNA is exposed to the cytoplasm due to the dissolved nuclear membrane. As cGAS are competitively bound by nucleosomes, it may lose the ability to bind dsDNA and activate the STING downstream[17–21].

1.4 We find that cisplatin treatment induces an cGAS-STING dependent immune responses in bladder cancers. Cisplatin related immune responses promote the secretion of cytokines such as INF-β, IL-6 in vitro and can recruit CD8 + T cells and dendritic cells(DCs) infiltration in mice tumor model. Cisplatin induced DNA damage can activate intracellular cGAS by producing dsDNA fragments and micronuclei. It can also dissociate cGAS from chromatin by distorting the structural of nucleosomes, and restore the ability of cGAS to bind dsDNA and then activate STING signal. Exploration the immune effects of cisplatin in bladder cancer can help us to understand the diverse mechanisms of cisplatin and provide the basis for the combination of cisplatin and immunotherapy.

2. Materials And Methods

2.1 Cell culture

Human muscle invasive bladder cancer cell lines T24, TCCSUP and UMUC-3, mouse derived bladder cell lines MB49, and 293T cell line were purchased from the Cell Bank of the Chinese Academy of Sciences (Shanghai, China). Short tandem repeat DNA profiling analysis were performed to ensure the stable and reliable of all cell lines during the experiments. T24, TCCSUP, UMUC-3 and MB49 cells were cultured in RPMI-1640 medium (Thermo Fisher Scientific, Inc.), and 293T cells were cultured in DMEM medium (Thermo Fisher Scientific, Inc.). Mediums mentioned before were pre-supplemented with 10% fetal bovine serum (Gibco; Thermo Fisher Scientific, Inc.) without any antibiotics, and all cell lines were incubated under standard conditions (37 °C and 5% CO_2).

2.2 Cell counting kit-8 (CCK-8) assay and Colony Formation assay

Each groups of T24, TCCSUP and MB49 cell lines were prepared in 96-well plates (1000 cells/well) under standard conditions. Then, premixed medium with a 10% concentration of CCK-8 (Dojindo Molecular Technologies, Inc., Kumamoto Japan) reagent was added into each well and incubated under standard conditions for 1–2 h before measurement at 450 nm. For colony formation assay, different groups of cells were prepared in 6-well plates (1000 cells/well) and cultured for 6–8 days under standard conditions followed by 3 min staining and 6 min fixation (Wright - Giemsa Stain Kit, NJJC bioengineering institution, China) at room temperature before colonies comparison.

2.3 Plasmids construction and transfection

Sequences of short hairpin RNA (shRNA) against CDS of msSTING were validated from Sigma-Aldrich Online. Scramble sequences were designed using Wizard v3.1 (https://www.invivogen.com/sirnawizard/) to ensure the absent of seed sequence matches. msSTING sequences and scramble sequences were synthesized (Tsingke, Hangzhou, China) and inserted into the plko.1-puro vector. Then the vector was co-transfected with pSPAX2 and pMD2G (with a ratio of 4: 3: 1, respectively) into the 293T cell lines cultured in 100 mm plates (30–60% cell density) using Lipofectamine 3000 (Thermo Fisher Scientific, Inc.) according to manufacturer's instruction. The supernatant, which contained Lentivirus, was harvested and centrifuged (800 × g, 5 min) 48 or 72 h post-transfection and added into MB49 cells cultured in 6-well plates (30–60% cell density) immediately. Successfully transfected shSTING cell lines were screened with an increasing concentration of puromycin (Sigma-Aldrich; Merck KGaA). The siRNA used here were also transfected using Lipofectamine 3000. Finally, the transfection efficiency was validated by western blotting. The msSTING and siSTING sequences used here were showed in Table S1.

2.4 Mice

C57BL/6 mice were purchased from Jackson Labs. 4 week mice were mainly used in this experiment and all mice were maintained in pathogen-free barrier facilities and were approved by Zhejiang University experimental animal welfare ethics review committee. 2×10^6 of MB49 cells with shSTING or shScr transfection were subcutaneous injected on the flank of mice. Then cisplatin (3 mg/kg) or PBS were injected subcutaneous injected around the tumors in day 13 and day 16. Tumors size were measured regularly by length (L), width (W) and height (H), respectively, and tumor volume was calculated as 1/2 ×

L × W × H. Then tumors were harvest in day 23, the weight of tumors were normalized by their corresponding body weight. Fresh tumor issues were then used for flow cytometry analysis.

2.5 RNA-sequence (RNA-seq) and Reverse transcription-quantitative polymerase chain reaction (RT-qPCR).

TRIzol (Thermo Fisher Scientific, Inc.) was used for cells total RNA extraction according to manufacturer's protocol. Then different groups of RNA were used for RNA-seq or qRT-PCR. T24 cells were treated with cisplatin (2 μg/ml) or PBS for 24 h at standard condition. RNA-sequence was performed by Novogene China. Gene expression levels were quantified as Fragments Per Kilobase Million and then Log_2 – transformed as A value. The significant different expression genes were identified as absolute fold change of A value > 1.5 combined Padj (adjust P) value < 0.05 between two groups. Then different expression genes were used for plotting heatmap and volcano map by R soltware (Version 4.0.2, https://cran.r-project.org/src/base/R-4/). GO and KEGG analysis were performed on DAVID online (https://david.ncifcrf.gov). Pathways with Padj value < 0.05 were identified as significant different pathway. As for qRT-PCR, Takara PrimeScript™ RT and SYBR EX Taq™ kits (Takara Bio, Inc., Otsu, Japan) were used for qRT-PCR according to manufacturer's instruction. The standard thermocycling conditions used were as follows: Initiate Step, 95.0 °C: 30 s; cycling Step, 40 cycles of 95 °C: 5 s and 60 °C: 30 s; melt curve analysis Step, 65 °C to 95 °C, increasing in 0.5 °C increments for 5 s. The specific primers used in this experiment were listed in Table S1. Control groups were conducted to confirm the absence of the agent pollution or primer dimers. Targeting genes were finally normalized to GAPDH expression, and the relative mRNA expressions were calculated using the ΔΔCq method.

2.6 Enzyme linked immunosorbent assay (ELISA) and IFN reporter assay

Secreted supernatant IL-6 of T24 and TCCSUP cell lines was measured using the Human IL-6 ELISA kit (DAKEWE, China) according to manufacturer’s instructions. IFN-β in cell supernatants with biological activity was compared using a reporter 293T cells stably expressing a pISRE (Genechem Co. Shanghai, China). Reporter cells were co-cultured with supernatant from different groups for 24 h before measured by a fluorescent enzyme meter Varioskan™ Flash at 488 nm/520 nm (Thermo Fisher Scientific, Inc.). Intensities of cellular fluorescent were normalized to the total number of T24 and TCCSUP cells.

2.7 Subcellular fractionation and Western blotting assay

Subcellular fractionation protein was extracted by Subcellular Protein Fractionation Kit for Cultured Cells (Thermo Fisher Scientific, Inc.) and NE-PER™ Nuclear and Cytoplasmic Extraction Reagents (Thermo Fisher Scientific, Inc.) according to the kit instruction. As for total protein extraction, T24, TCCSUP and MB49 cells were washed using cold PBS before being lysed using RIPA Lysis buffer with 1% cocktail protease inhibitor (Thermo Fisher Scientific, Inc.). After ultrasonic spallation at 4 °C, the protein samples were purified by centrifugation (4 °C, 15,000 × g, 15 min) and the clear supernatant extracts were quantification using a BCA protein assay (Thermo Fisher Scientific, Inc.) and 25 μg/10 μl denatured

protein samples were prepared and loaded in 4–12% Tris-acetate gels (Invitrogen; Thermo Fisher Scientific, Inc.) and then separated by electrophoresis. Then, the proteins were transferred onto a polyvinylidene fluoride membrane with 0.45 μm pore size. Then, the membrane was blocked with 5% bovine serum albumin (BSA, Fdbio Science, Hangzhou, China) in Tris-buffered saline containing 1% Tween-20 (TBST) for 1 h at room temperature and further incubated with primary antibodies for 12 h in a shaker at 4 °C. Subsequent to washing with TBST 5 min for three times, the membrane was incubated with secondary antibodies for 1 h at room temperature. The information of abovementioned primary antibodies: Human-Reactive STING Pathway Antibody Sampler Kit (1:1, 000; cat no. #38866; Cell signaling technology, CST), Mouse-Reactive STING Pathway Antibody Sampler Kit (1:1, 000; cat no. #16029; CST), γ-H2A.X (1:1, 000; cat no. ab81299; Abcam), Rad51(1:1, 000; cat no. ab133534; Abcam), GAPDH (1:5, 000; cat no. ab8245; Abcam) and Histone H3 (1:1, 000; cat no. ab1791; Abcam). The information of abovementioned secondary antibodies: Goat anti Rabbit- HRP (1: 3, 000; cat no. PDR007; Fdbio Science) and Goat anti Mouse-HRP (1: 3, 000; cat no. PDM007; Fdbio Science). The blotting results were illustrated by Dura ECL detection kit (Fdbio Science) and specific protein bands were analyzed using Image-Pro Plus software 6.0 (Media Cybernetics, Inc., Rockville, MD, USA). GAPDH was selected as a total control protein or cytosolic control protein, histone H3 was selected as total nuclear control protein or chromatin bound control protein.

2.8 Flow cytometry analysis

Tumor tissues were digested and incubated with biotinylated anti-CD3, anti-CD8 antibodies, followed by incubated with streptavidin-PE/Cy7 (Cat no.SA1012; Invitrogen™), anti-CD45.2-APC for 10 min at room temperature in darkroom. For analyzing DCs, tissue cells were incubated with anti-MHC□-APC and anti-CD11c-PE for 10 min at room temperature in darkroom. To analyze macrophage cells, tumor cells was collected and stained with anti-CD11b-APC and anti-F4/80-PE for 10 min at room temperature in darkroom. The antibodies used in flow cytometry analysis were: anti-CD3 (1:200; cat no. 13-0032-82; eBioscience™), anti-CD8 (1:200; cat no. 13-0081-82; eBioscience™), anti-CD45.2-APC (1:200; cat no. 17-0454-82; eBioscience™), anti-MHC□-APC (1:200; cat no. 17-5321-82; eBioscience™), anti-CD11c-PE (1:200; cat no. 12-0114-82; eBioscience™), anti-CD11b-APC (1:200; cat no. 17-0112-82, eBioscience™) and anti-F4/80-PE (1:200; cat no. 17-4801-82; eBioscience™).Then the infiltration percentages of different cell types in tumors were calculated by BD FACSCanto™ II (BD Biosciences) and then analyzed by FlowJo 10.0 (FlowJo LLC, Ashland, OR, USA).

2.9 Immunofluorescence

Different groups of T24, TCCSUP, UMUC-3 and MB49 cells were pre-seeded the day before immunofluorescence assay. 4% paraformaldehyde was used for cell fixation and 0.5% Triton-X 100 was used to increase cell membrane permeability for 10–15 min at room temperature. Then 3–5% BSA was used for 30–60 min at room temperature to block antibodies. Cells were further incubated with primary antibodies overnight at 4 °C and subsequently incubated with corresponding fluorescence antibodies combined with DAPI staining 30–60 min in darkroom and then wash twice by PBS before observed by NIS A1 laser confocal microscope (Nikon, Japan). The primary antibodies used for immunofluorescence

assay were: cGAS (1:200; cat no. A8335; Abclonal), F-actin (1:1, 000; cat no. A12380; Invitrogen™), Rad51(1:300; cat no. ab133534; Abcam), γ-H2A.X (1:300; cat no. ab81299; Abcam). The secondary antibodies used for immunofluorescence assay were: Goat Anti-Rabbit Alexa Fluor 488 (1:200; cat no. ab150077; Abcam) and Goat Anti-Mouse Alexa Fluor 594 (1:200; cat no. ab150116; Abcam). The results were analyzed by NIS-Elements Viewer 4.50 (Nikon, Japan).

2.10 Statistical analysis

SPSS 22.0 (IBM Corp. USA) was used to normalize and analyze raw data in this experiment. Data was presented as the mean ± standard deviation. Kaplan-Meier survival method and log-rank test analysis were using to plot (OS) overall survival and (DFS) disease-free survival rates curves. A student's t-test was used to assess the different between two groups. One-way ANOVA test was performed to assess the differences in multiples groups followed by Student-Newman-Keuls post hoc test. IC50 of MB49 cell lines were measured by Probit regression analysis. $P < 0.05$ was considered to have statistical significance. Data in experiments was repeated at least 3 times.

3. Results

3.1 Cisplatin induces specific immune effects in bladder cancer cell line.

In order to explore the specific effect of cisplatin on bladder cancer, a MIBC derived cell line T24 was treated with cisplatin (2 μg/ml, 24 h) followed by RNA SEq. We found a significant difference gene expression panels between cisplatin treated groups and control groups (Fig. 1A). The combination of absolute value $\log_2$(Fold Change) > 1.5 and Padj (adjust P) value < 0.05 was chosen as the criteria for screening significant differential genes between two groups, and finally we got 235 up-regulated and 129 down regulated genes (Fig. 1B). After GO and KEGG (https://david.ncifcrf.gov) analysis of these differentially expressed genes, we found that the treatment of cisplatin mainly affect T24 cells in immune response, inflammatory response, cytokine activity, the cellular response to DNA damage stimulus, apoptosis process and some cell growth related pathways (Fig. 1C). Gene set enrichment analysis (GSEA) also confirmed the strong enrichment in immune- and inflammation-related pathways among the top 20 differentially expressed pathways in cisplatin treated group. Interestingly, we noticed type I interferon related pathway and cytosolic DNA sensor pathway were significantly up-regulated after cisplatin stimulation (Fig. 1D, Figure S1B, C). The involved cellular response to cytosolic DNA sensor process is closely relevant to cGAS-STING pathway. Recently, it has been reported that cGAS, an intracellular dsDNA receptor, can recognize and catalysis dsDNA induced by cisplatin, thus activating the downstream STING pathway[4]. Then, we explored the activation of cGAS-STING downstream and found that transcription levels of NF-κB and IRF3 related genes were significantly up-regulated after cisplatin treatment (Fig. 1E). These results suggest that the immune effects associated with cisplatin are on account of the activation of cGAS-STING pathway[4, 11].

3.2 The immune effect of cisplatin in bladder cancer is related to the activation of cGAS-STING pathway.

Expression of STING protein is the basic element for functional STING pathway. We firstly explored the basic transcription level of STING in bladder cancer cell lines in CCLE database (https://portals.broadinstitute.org/ccle/about), and found that the transcription level of STING was relative abundant in bladder cancer, including T24 another MIBC cell line TCCSUP cell lines (Fig. 2A). In both ELISA and INF-β reporter gene assay we found the levels of IL-6 and INF-β, the activated downstream of STING pathway, were significantly up-regulated with cisplatin treatment in T24 and TCCSUP (Fig. 2A, B). It was confirmed by qPCR that the transcription levels of cytokines including IL-6, INF-β and TNF-α were significantly up-regulated after cisplatin treatment (Fig. 2D). We also observed the translocation of p65 from cytoplasm to nuclear (Fig. 2E). The canonical activation of STING pathway is mainly based on the phosphorylate of STING (Ser366), TBK (Ser173) and IRF3 (Ser396)[22–24]. We then performed Western blotting assay and found that the cisplatin treatment significantly up-regulated cGAS-STING pathway accompanied by a significant increase of DNA damage marker γ-H2A.X in two cell lines, compared with their corresponding control groups (Fig. 2F). The polymer state of STING is the activated result of phosphorylated STING[10,25], we found the polymer of STING and γ-H2A.X were increased with the time of cisplatin stimulation expanded (Figure S1A). We also noticed that the cell surface PD-L1 level of two cell lines increased significantly with cisplatin inducing (Fig. 2G). In rescue assay, the use of two STING targeting siRNAs (Fig. 3A-C) and STING specific inhibitor H151 (Fig. 3D, E) significantly reversed cisplatin induced IL-6 and INF-β levels compared with their control groups, respectively. These results suggested that cGAS-STING pathway was deeply involved in cisplatin related immune response.

3.3 Modulation of STING did not affect the proliferation of bladder cancer in vitro.

Since cisplatin activates cGAS-STING signal in bladder cancer cell lines, what role does cGAS-STING plays in bladder cancer progression remains unclear. The CCK8 cell proliferation assay (Fig. 4A) and clonal formation assay indicated the absence of significant basic proliferation bias between STING knockdown groups and control groups in two cell lines (Fig. 4D, E). We found that the levels of cGAS-STING pathway related key genes in patients from TCGA bladder cancer cohort were not significantly associated with overall survival rate (OS) and disease free survival rate (DFS) (Fig. 4B, C; Figure S1D-I). This imply that the activation states and expression levels of genes in cGAS-STING pathway is not inevitable relevant.

3.4 Activation of cGAS-STING suppressed bladder cancer in cisplatin-treated C57 mice.

In order to explore the phenotype in vivo, we constructed a MB49 shSTING cell line and a MB49 scramble control cell line (Mouse derived) by lentivirus transfection (Fig. 4F). To exclude the possible effects caused by different cell proliferation rate and cisplatin sensitivity between two constructed cell lines, we

verified before that there was no significant difference existed in cell proliferation (Fig. 4G, I, J) and basic IC50 of cisplatin treatment in two groups (Fig. 4H). At the same time, we noticed that cisplatin treatment activated cGAS-STING signal in MB49 scramble control group but not MB49 STING knockdown groups (Fig. 4K). We then establish the subcutaneous tumor transplantation model in C57 mice, cisplatin or PBS was injected subcutaneous in day 13 and day 19 (Fig. 5A-left). The tumors were harvest in day 23, and the results showed that the tumor volumes in the cisplatin treated group was significantly reduced compared with the corresponding control group (Fig. 5A-right). Compared with STING knockdown group, the tumor volume and relative tumor weight of STING WT group were significantly reduced after cisplatin treatment (Figure S2 A-C).

3.5 Activation of cGAS-STING results in the CD8 + T cells and DCs infiltration in cisplatin-treated tumors in xenograft transplantation model.

In order to explore whether the difference in MB49 derived tumor is related to immunity, we analyzed tumor associated infiltrating immune cells by flow cytometry. With cisplatin treatment, we found that compared with STING knockdown group, the percentage of CD8 + CD45+, CD11c + MHCII+ (Dendritic cells, DCs), CD3 + CD45 + was significantly higher in STING WT group (Fig. 5B, C, E), but the percentage of F4/80+, CD11b+ (Macrophage) infiltration was not significantly different (Fig. 5D). Compared with the control group, the percentage of CD8 + CD45+, CD3 + CD45+, F4/80 + CD11b + in cisplatin treated groups decreased significantly, but the percentage of CD11c + MHCII + infiltration cells were significantly increased. Studies have reported that CCL20 and CXCL14 are important chemokines for DCs cells. We found that the transcription levels of CCL20 and CXCL14 in T24 and TCCSUP cells were significantly increased in cisplatin treatment groups (Figure S2D, E), correlation analysis showed that CCL20 and CXCL14 were significantly correlated with cGAS-STING signal in TCGA bladder cancer cohort (Figure S2F). We also performed CIBERSORT (https://cibersort.stanford.edu) to analyzed the percentage of immune cell infiltration in patients with bladder cancer who received cisplatin based chemotherapy in TCGA bladder cancer cohort (https://portal.gdc.cancer.gov/)[26](Figure S3A-C). Interestingly, we found that the infiltration of DCs activated cells in response group (n = 50, CR or PR) was significantly lower than non-response group (n = 30, PD or SD) after cisplatin based chemotherapy, while the infiltration of DCs resting cells in two groups displayed the opposite results (Fig. 5F-I). This finding imply that a unique role that DCs paly in bladder cancer microenvironment after cisplatin treatment[27]. However, the specific function of cisplatin induced DCs in bladder cancer microenvironment needs to be further explored.

3.6 Cisplatin induced dsDNA may function as an important role in enhancing STING signal.

As an important protein that can recognize dsDNA and catalyze the production of 2, 3 - cGAMPs, expression of cGAS protein is the most important upstream of STING activation. We then explored the basic transcription level of cGAS in bladder cancer cell lines in CCLE database

(https://portals.broadinstitute.org/ccle/about), and confirmed the high transcription level of cGAS in bladder cancer cell lines (rank 11th among 40 tumor types), and T24 and TCCSUP also showed relative high transcription levels of cGAS (Fig. 6A, Figure S3D). It was reported that cisplatin induced dsDNA fragments through accumulation of DNA damage and inhibiting DNA homologous complementary repair pathway[16]. We observed the significant increase of DNA damage marker γ-H2A.X in T24 and TCCSUP cell lines treated with cisplatin (Fig. 2F). Rad51 is an important protein involved in homologous complementary repair of DNA, the up-regulated and assembled of nuclear Rad51 is also the classical marker of increased DNA damage[28]. We found nuclear Rad51 increased and assembled significantly after cisplatin stimulation while the cytosolic Rad51 levels was not changed (Fig. 6C, D). When dsDNA induced by DNA damage leaks into the cytoplasm, histone H3 bound to dsDNA will be brought into the cytoplasm in the same time, resulting in an increase level of cytosolic H3 protein[29]. In consistent with our results, we observed that the level of H3 in the cytoplasm increased significantly with the time of cisplatin stimulation expand (Fig. 5A, B), which also suggested that dsDNA might leak from the nucleus continuously after cisplatin treatment. Furthermore, we found that cisplatin also induced micronuclei in T24 and TCCSUP cell lines (Figure S3E). These are important factors to activate cGAS-STING pathway.

3.7 The release of chromatin bound cGAS is important to activate downstream STING.

We tried to explore the role of cGAS in cisplatin related STING activation and found that the expression level of total cGAS did not change significantly after cisplatin stimulation in two cell lines (Fig. 2E). The subcellular distribution of cGAS is closely related to its function[17–21]. At first we confirmed that cGAS protein of T24 and TCCSUP cell lines was mainly located in nucleus (Fig. 6C, E). And same results were also showed in MB49 and UMUC3 cell lines (Fig. 6E). Then we tried to explore whether the subcellular distribution of cGAS was changed after the cisplatin treatment. Though the morphology of T24 and TCCSUP cells became enlarged after cisplatin stimulation, the distribution of cGAS did not change significantly (Fig. 6F). Western blotting results of nuclear-cytoplasmic separation also showed that cGAS distribution in cytoplasm and nucleus did not change significantly in two cell lines (Fig. 6C). Recently, many scholars have found that cGAS can bind with histones H2 and H3 on nucleosome to form stable structure and prevent cGAS from binding with dsDNA[17–21]. Based on this findings, we performed subcellular component western blotting assay and found that most of cGAS were bound to the nucleosome in the nucleus. After cisplatin stimulation, especially at 24 h, the binding of cGAS in nucleosome in two cell lines was significantly reduced accompanied by a significant increase of γ-H2A.X, compared with their corresponding control groups (Fig. 6G). Thus the free cGAS might reacquire the ability to bind to dsDNA and then activate downstream STING dependent immune signal.

4. Discussion

4.1 In this work, we reported that cisplatin treatment of bladder cancer cells did produce specific immune effects, mainly including the secretion of important cytokines (such as interferon type I cytokines, INF-β, IL6) and the increase of PD-L1 level on the cell surface. Recently, the remarkable keynote 189 trials

showed that platinum based chemotherapy combined with PD1 showed better prognosis than chemotherapy alone in non-small cell lung cancer. We then confirmed that cGAS-STING signal were deeply involved in these immune effects. Cisplatin relative cGAS-STING signals have also been reported in ovarian cancer, NSCLC and epithelial cell carcinoma[30–31]. These results provided the potential therapeutic choice of combined cisplatin and immune therapy in bladder cancer therapy.

4.2 The expression levels of STING and other components involved in STING pathway were not associated with OS and DFS in bladder cancer patients. But in mice tumor model, we confirmed that knockdown of STING in bladder cell had no significant effect on tumor volume and weight, but the tumor volume and weight in group of STING-knockdown combined cisplatin treatment was significantly larger than in group of STING WT combined cisplatin treatment. These results suggest that cisplatin related STING dependent signal strong inhibits bladder cancer progression, which is consistent with many previous studies[7–9, 30, 31]. These difference might be explained by higher infiltration levels of CD8 + T cells and DCs cells in STING-WT combined with cisplatin group, compared with that in STING-knockdown combined with cisplatin group. The infiltration levels of CD8 + T cells in tumor tissues is recently proved to be consistent with functional cGAS-STING pathway[32]. The infiltration and activation of DCs cells in tumor tissues is closely related to specific chemokines in tumor microenvironment. Chemokines like CCL20 and CXCL14 can recruit DCs to tumor tissue to inhibit tumor proliferation and metastasis[33,34]. In our experiment, we also observed the increased transcription levels of CCL20 and CXCL14 in T24 and TCCSUP cell lines after cisplatin treatment. It is also reported that intrinsic cGAMPs in tumor cells can be transferred to DCs through gap junction and activate the immune response of DCs cells[35,36]. By CIBERSORT analysis, we predicted that the infiltration percentage of DCs activated cells in response group (n = 50, CR or PR) was significantly lower than unresponse group (n = 30, PD or SD) in patient receiving platinum based chemotherapy in TCGA bladder cancer cohort. Thus, DCs may play an important role in cisplatin related cGAS-STING immune effects in bladder cancer, but its underlying mechanism and specific functions towards tumor microenvironment remain to be clarified.

4.3 Urinary tract tumors including bladder cancer has relative high expression of cGAS. Researches have shown that tumor cells with high expression of cGAS protein have relatively active cGAS-STING pathway activity[35]. This is because that tumor cells often have higher levels of intracellular dsDNA due to more frequent DNA damage and repair cycles, which can activate cGAS and generate plenty of cGAMPs and finally activate STING downstream[35,36]. As a classical DNA crosslinking agent, cisplatin can strongly induce DNA damage in multiple tumor types. DNA damage lead to dsDNA leakage from nucleus to cytoplasm[4,5,29]. We observed that with the time of cisplatin inducing expand, the level of histone H3 in cytoplasm increased gradually, which indicated that dsDNA was constantly leaking from the nucleus[29]. At the same time, we observed the production of micronuclei in cisplatin treated groups. Micronuclei was reported not only as a marker of DNA damage, but also as a way to activate STING signal[5].

4.4 The functional state of cGAS is closely related to its subcellular localization. For instance, translocation of cGAS from cytoplasm to cell membrane helps THP-1 and HeLa cells to recognize the

exogenous virus DNA[37]. And nuclear translocation of cGAS can affect its functions by suppressing homologous recombination mediated repair[16]. But we found that cGAS was mainly located in nucleus in T24 and TCCSUP cell lines, and this subcellular distribution was not changed after cisplatin treatment. Studies have shown that the binding capacity of cGAS to nucleosomes is much greater than that of cGAS to dsDNA[17–21, 38]. Based on this important finding, many research groups further discovery that cGAS can bind with histones H2 and H3 on nucleosome to form stable structure and prevent cGAS from binding with dsDNA[17–21]. So, we then explored the state of chromatin binding cGAS after cisplatin treatment, and found that with the prolongation of cisplatin treatment, the DNA damage marker γ-H2A.X increased significantly, while the chromatin bound cGAS decreased significantly. In multiple tumor types, the activation of cGAS is thought to have the function of inhibiting tumor proliferation by activating STING dependent immune response, but this function will be weakened due to the binding of nucleosome[7–9]. These results indicate that cisplatin may hamper the stability of nucleosome by distorting the natural structural of DNA[39,40]. The free cGAS may reacquire the ability to bind to dsDNA and then activate downstream STING dependent immune signal. However, whether the dissociated cGAS is transferred to the cytoplasm and further activate STING still need to be proved.

5. Conclusion

In summary, our findings indicated a cisplatin dependent cGAS-STING signal in bladder cancer. This signal could be enhanced by accumulation of dsDNA and chromatin dissociated cGAS and would finally recruit infiltration DCs and CD8 + T cells in bladder cancer bladder cancer tumor microenvironment. However, the specific role and effect of this signal towards bladder cancer tumor microenvironment need to be further clarified.

Abbreviations

cGAMPs
Cyclic GMP–AMPs
cGAS
Cyclic GMP–AMP synthase
DCs
Dendritic cells
IRF3
Interferon regulatory factor 3
MIBC
Muscle invasive bladder cancer
NMIBC
Non-muscle invasive bladder cancer
STING
Stimulator of interferon genes

TBK1
TANK-binding kinase 1

Declarations

Ethics approval and consent to participate: Not applicable.

Consent for publication: Not applicable.

Availability of data and material: The datasets used and/or analyzed during the current study are available from the corresponding author on reasonable request.

Competing interests: The authors declare that they have no competing interests.

Funding: This work was supported by the Key Projects of Science and Technology Department of Zhejiang Province (grant no. 2020C03026) and Zhejiang Provincial Natural Science Foundation of China (grant no. LQ21H160019).

Authors' contributions: GF and BJ designed the experiments, performed the experiments. XC and XZ analyzed the data and wrote the paper. CX, JS, JT and YS performed the experiments. FZ, YW and HP provided the reagents and helped with the experiments and the writing of the paper. All authors read and approved the final manuscript.

Acknowledgements

Thank Doctor Dan Huang for her help in animal experiments and plasmid construction.

References

1. Siegel RL, Miller KD, Jemal A. Cancer statistics, 2019. CA Cancer J Clin. 2019 Jan;69(1):7-34. doi: 10.3322/caac.21551. Epub 2019 Jan 8. PMID: 30620402.
2. Galsky MD, Chen GJ, Oh WK, Bellmunt J, Roth BJ, Petrioli R, Dogliotti L, Dreicer R, Sonpavde G. Comparative effectiveness of cisplatin-based and carboplatin-based chemotherapy for treatment of advanced urothelial carcinoma. Ann Oncol. 2012 Feb;23(2):406-10. doi: 10.1093/annonc/mdr156. Epub 2011 May 4. PMID: 21543626.
3. Alfred Witjes J, Lebret T, Compérat EM, Cowan NC, De Santis M, Bruins HM, Hernández V, Espinós EL, Dunn J, Rouanne M, Neuzillet Y, Veskimäe E, van der Heijden AG, Gakis G, Ribal MJ. Updated 2016 EAU Guidelines on Muscle-invasive and Metastatic Bladder Cancer. Eur Urol. 2017 Mar;71(3):462-475. doi: 10.1016/j.eururo.2016.06.020. Epub 2016 Jun 30. PMID: 27375033.
4. Rycenga HB, Long DT. The evolving role of DNA inter-strand crosslinks in chemotherapy. Curr Opin Pharmacol. 2018 Aug; 41:20-26. doi: 10.1016/j.coph.2018.04.004. Epub 2018 Apr 18. PMID: 29679802; PMCID: PMC6108900.

5. Jiang H, Xue X, Panda S, Kawale A, Hooy RM, Liang F, Sohn J, Sung P, Gekara NO. Chromatin-bound cGAS is an inhibitor of DNA repair and hence accelerates genome destabilization and cell death. EMBO J. 2019 Oct 4;38(21):e102718. doi: 10.15252/embj.2019102718. Epub 2019 Sep 23. PMID: 31544964; PMCID: PMC6826206.
6. Gandhi L, Rodríguez-Abreu D, Gadgeel S, Esteban E, Felip E, De Angelis F, Domine M, Clingan P, Hochmair MJ, Powell SF, Cheng SY, Bischoff HG, Peled N, Grossi F, Jennens RR, Reck M, Hui R, Garon EB, Boyer M, Rubio-Viqueira B, Novello S, Kurata T, Gray JE, Vida J, Wei Z, Yang J, Raftopoulos H, Pietanza MC, Garassino MC; KEYNOTE-189 Investigators. Pembrolizumab plus Chemotherapy in Metastatic Non-Small-Cell Lung Cancer. N Engl J Med. 2018 May 31;378(22):2078-2092. doi: 10.1056/NEJMoa1801005. Epub 2018 Apr 16. PMID: 29658856.
7. Ng KW, Marshall EA, Bell JC, Lam WL. cGAS-STING and Cancer: Dichotomous Roles in Tumor Immunity and Development. Trends Immunol. 2018 Jan;39(1):44-54. doi: 10.1016/j.it.2017.07.013. Epub 2017 Aug 19. PMID: 28830732.
8. Grabosch S, Bulatovic M, Zeng F, Ma T, Zhang L, Ross M, Brozick J, Fang Y, Tseng G, Kim E, Gambotto A, Elishaev E, P Edwards R, Vlad AM. Cisplatin-induced immune modulation in ovarian cancer mouse models with distinct inflammation profiles. Oncogene. 2019 Mar;38(13):2380-2393. doi: 10.1038/s41388-018-0581-9. Epub 2018 Dec 5. PMID: 30518877; PMCID: PMC6440870.
9. Nolan E, Savas P, Policheni AN, Darcy PK, Vaillant F, Mintoff CP, Dushyanthen S, Mansour M, Pang JB, Fox SB; Kathleen Cuningham Foundation Consortium for Research into Familial Breast Cancer (kConFab), Perou CM, Visvader JE, Gray DHD, Loi S, Lindeman GJ. Combined immune checkpoint blockade as a therapeutic strategy for BRCA1-mutated breast cancer. Sci Transl Med. 2017 Jun 7;9(393):eaal4922. doi: 10.1126/scitranslmed. aal4922. PMID: 28592566; PMCID: PMC5822709.
10. Sun L, Wu J, Du F, Chen X, Chen ZJ. Cyclic GMP-AMP synthase is a cytosolic DNA sensor that activates the type I interferon pathway. Science. 2013 Feb 15;339(6121):786-91. doi: 10.1126/science.1232458. Epub 2012 Dec 20. PMID: 23258413; PMCID: PMC3863629.
11. Chen Q, Sun L, Chen ZJ. Regulation and function of the cGAS-STING pathway of cytosolic DNA sensing. Nat Immunol. 2016 Sep 20;17(10):1142-9. doi: 10.1038/ni.3558. PMID: 27648547.
12. Pei J, Zhang Y, Luo Q, Zheng W, Li W, Zeng X, Li Q, Quan J. STAT3 inhibition enhances CDN-induced STING signaling and antitumor immunity. Cancer Lett. 2019 May 28; 450:110-122. doi: 10.1016/j.canlet.2019.02.029. Epub 2019 Feb 18. PMID: 30790684. 13. Ahn J, Konno H, Barber GN. Diverse roles of STING-dependent signaling on the development of cancer. Oncogene. 2015 Oct 8;34(41):5302-8. doi: 10.1038/onc.2014.457. Epub 2015 Feb 2. PMID: 25639870; PMCID: PMC4998969.
13. Wang S, Wang L, Qin X, Turdi S, Sun D, Culver B, Reiter RJ, Wang X, Zhou H, Ren J. ALDH2 contributes to melatonin-induced protection against APP/PS1 mutation-prompted cardiac anomalies through cGAS-STING-TBK1-mediated regulation of mitophagy. Signal Transduct Target Ther. 2020 Jul 24;5(1):119. doi: 10.1038/s41392-020-0171-5. PMID: 32703954; PMCID: PMC7378833.

14. Abe T, Barber GN. Cytosolic-DNA-mediated, STING-dependent proinflammatory gene induction necessitates canonical NF-κB activation through TBK1. J Virol. 2014 May;88(10):5328-41. doi: 10.1128/JVI.00037-14. Epub 2014 Mar 5. PMID: 24600004; PMCID: PMC4019140.
15. Liu H, Zhang H, Wu X, Ma D, Wu J, Wang L, Jiang Y, Fei Y, Zhu C, Tan R, Jungblut P, Pei G, Dorhoi A, Yan Q, Zhang F, Zheng R, Liu S, Liang H, Liu Z, Yang H, Chen J, Wang P, Tang T, Peng W, Hu Z, Xu Z, Huang X, Wang J, Li H, Zhou Y, Liu F, Yan D, Kaufmann SHE, Chen C, Mao Z, Ge B. Nuclear cGAS suppresses DNA repair and promotes tumorigenesis. Nature. 2018 Nov;563(7729):131-136. doi: 10.1038/s41586-018-0629-6. Epub 2018 Oct 24. PMID: 30356214.
16. Boyer JA, Spangler CJ, Strauss JD, Cesmat AP, Liu P, McGinty RK, Zhang Q. Structural basis of nucleosome-dependent cGAS inhibition. Science. 2020 Oct 23;370(6515):450-454. doi: 10.1126/science.abd0609. Epub 2020 Sep 10. PMID: 32913000.
17. Kujirai T, Zierhut C, Takizawa Y, Kim R, Negishi L, Uruma N, Hirai S, Funabiki H, Kurumizaka H. Structural basis for the inhibition of cGAS by nucleosomes. Science. 2020 Oct 23;370(6515):455-458. doi: 10.1126/science.abd0237. Epub 2020 Sep 10. PMID: 32912999; PMCID: PMC7584773.
18. Pathare GR, Decout A, Glück S, Cavadini S, Makasheva K, Hovius R, Kempf G, Weiss J, Kozicka Z, Guey B, Melenec P, Fierz B, Thomä NH, Ablasser A. Structural mechanism of cGAS inhibition by the nucleosome. Nature. 2020 Sep 10. doi: 10.1038/s41586-020-2750-6. Epub ahead of print. PMID: 32911482.
19. Zhao B, Xu P, Rowlett CM, Jing T, Shinde O, Lei Y, West AP, Liu WR, Li P. The molecular basis of tight nuclear tethering and inactivation of cGAS. Nature. 2020 Sep 10. doi: 10.1038/s41586-020-2749-z. Epub ahead of print. PMID: 32911481.
20. Michalski S, de Oliveira Mann CC, Stafford CA, Witte G, Bartho J, Lammens K, Hornung V, Hopfner KP. Structural basis for sequestration and autoinhibition of cGAS by chromatin. Nature. 2020 Sep 10. doi: 10.1038/s41586-020-2748-0. Epub ahead of print. PMID: 32911480.
21. Liu S, Cai X, Wu J, Cong Q, Chen X, Li T, Du F, Ren J, Wu YT, Grishin NV, Chen ZJ. Phosphorylation of innate immune adaptor proteins MAVS, STING, and TRIF induces IRF3 activation. Science. 2015 Mar 13;347(6227):aaa2630. doi: 10.1126/science.aaa2630. Epub 2015 Jan 29. PMID: 25636800.
22. Zhang C, Shang G, Gui X, Zhang X, Bai XC, Chen ZJ. Structural basis of STING binding with and phosphorylation by TBK1. Nature. 2019 Mar;567(7748):394-398. doi: 10.1038/s41586-019-1000-2. Epub 2019 Mar 6. PMID: 30842653; PMCID: PMC6862768.
23. Fitzgerald KA, McWhirter SM, Faia KL, Rowe DC, Latz E, Golenbock DT, Coyle AJ, Liao SM, Maniatis T. IKKepsilon and TBK1 are essential components of the IRF3 signaling pathway. Nat Immunol. 2003 May;4(5):491-6. doi: 10.1038/ni921. PMID: 12692549.
24. Ergun SL, Fernandez D, Weiss TM, Li L. STING Polymer Structure Reveals Mechanisms for Activation, Hyperactivation, and Inhibition. Cell. 2019 Jul 11;178(2):290-301.e10. doi: 10.1016/j.cell.2019.05.036. Epub 2019 Jun 20. PMID: 31230712.
25. Newman AM, Liu CL, Green MR, Gentles AJ, Feng W, Xu Y, Hoang CD, Diehn M, Alizadeh AA. Robust enumeration of cell subsets from tissue expression profiles. Nat Methods. 2015 May;12(5):453-7.

doi: 10.1038/nmeth.3337. Epub 2015 Mar 30. PMID: 25822800; PMCID: PMC4739640.

26. Zhang Q, Chen Z. Sensitization of cisplatin resistant bladder tumor by combination of cisplatin treatment and co-culture of dendritic cells with apoptotic bladder cancer cells. Cell Mol Biol (Noisy-le-grand). 2018 Jul 30;64(10):102-107. PMID: 30084800.
27. Nacson J, Di Marcantonio D, Wang Y, Bernhardy AJ, Clausen E, Hua X, Cai KQ, Martinez E, Feng W, Callén E, Wu W, Gupta GP, Testa JR, Nussenzweig A, Sykes SM, Johnson N. BRCA1 Mutational Complementation Induces Synthetic Viability. Mol Cell. 2020 Jun 4;78(5):951-959.e6. doi: 10.1016/j.molcel.2020.04.006. Epub 2020 Apr 30. PMID: 32359443; PMCID: PMC7418109.
28. Parkes EE, Walker SM, Taggart LE, McCabe N, Knight LA, Wilkinson R, McCloskey KD, Buckley NE, Savage KI, Salto-Tellez M, McQuaid S, Harte MT, Mullan PB, Harkin DP, Kennedy RD. Activation of STING-Dependent Innate Immune Signaling By S-Phase-Specific DNA Damage in Breast Cancer. J Natl Cancer Inst. 2016 Oct 5;109(1):djw199. doi: 10.1093/jnci/djw199. PMID: 27707838; PMCID: PMC5441301.
29. Grabosch S, Bulatovic M, Zeng F, Ma T, Zhang L, Ross M, Brozick J, Fang Y, Tseng G, Kim E, Gambotto A, Elishaev E, P Edwards R, Vlad AM. Cisplatin-induced immune modulation in ovarian cancer mouse models with distinct inflammation profiles. Oncogene. 2019 Mar;38(13):2380-2393. doi: 10.1038/s41388-018-0581-9. Epub 2018 Dec 5. PMID: 30518877; PMCID: PMC6440870.
30. Della Corte CM, Sen T, Gay CM, Ramkumar K, Diao L, Cardnell RJ, Rodriguez BL, Stewart CA, Papadimitrakopoulou VA, Gibson L, Fradette JJ, Wang Q, Fan Y, Peng DH, Negrao MV, Wistuba II, Fujimoto J, Solis Soto LM, Behrens C, Skoulidis F, Heymach JV, Wang J, Gibbons DL, Byers LA. STING Pathway Expression Identifies NSCLC With an Immune-Responsive Phenotype. J Thorac Oncol. 2020 May;15(5):777-791. doi: 10.1016/j.jtho.2020.01.009. Epub 2020 Feb 15. PMID: 32068166; PMCID: PMC7202130.
31. Li T, Chen ZJ. The cGAS-cGAMP-STING pathway connects DNA damage to inflammation, senescence, and cancer. J Exp Med. 2018 May 7;215(5):1287-1299. doi: 10.1084/jem.20180139. Epub 2018 Apr 5. PMID: 29622565; PMCID: PMC5940270.
32. Fushimi T, Kojima A, Moore MA, Crystal RG. Macrophage inflammatory protein 3alpha transgene attracts dendritic cells to established murine tumors and suppresses tumor growth. J Clin Invest. 2000 May;105(10):1383-93. doi: 10.1172/JCI7548. PMID: 10811846; PMCID: PMC315459.
33. Shurin GV, Ferris RL, Tourkova IL, Perez L, Lokshin A, Balkir L, Collins B, Chatta GS, Shurin MR. Loss of new chemokine CXCL14 in tumor tissue is associated with low infiltration by dendritic cells (DC), while restoration of human CXCL14 expression in tumor cells causes attraction of DC both in vitro and in vivo. J Immunol. 2005 May 1;174(9):5490-8. doi: 10.4049/jimmunol.174.9.5490. Erratum in: J Immunol. 2006 Mar 15;176(6):3840. Ferris, Robert [corrected to Ferris, Robert L]. PMID: 15843547.
34. Schadt L, Sparano C, Schweiger NA, Silina K, Cecconi V, Lucchiari G, Yagita H, Guggisberg E, Saba S, Nascakova Z, Barchet W, van den Broek M. Cancer-Cell-Intrinsic cGAS Expression Mediates Tumor Immunogenicity. Cell Rep. 2019 Oct 29;29(5):1236-1248.e7. doi: 10.1016/j.celrep.2019.09.065. PMID: 31665636.

35. Saccheri F, Pozzi C, Avogadri F, Barozzi S, Faretta M, Fusi P, Rescigno M. Bacteria-induced gap junctions in tumors favor antigen cross-presentation and antitumor immunity. Sci Transl Med. 2010 Aug 11;2(44):44ra57. doi: 10.1126/scitranslmed.3000739. PMID: 20702856.
36. Barnett KC, Coronas-Serna JM, Zhou W, Ernandes MJ, Cao A, Kranzusch PJ, Kagan JC. Phosphoinositide Interactions Position cGAS at the Plasma Membrane to Ensure Efficient Distinction between Self- and Viral DNA. Cell. 2019 Mar 7;176(6):1432-1446.e11. doi: 10.1016/j.cell.2019.01.049. Epub 2019 Feb 28. PMID: 30827685; PMCID: PMC6697112.
37. Zierhut C, Yamaguchi N, Paredes M, Luo JD, Carroll T, Funabiki H. The Cytoplasmic DNA Sensor cGAS Promotes Mitotic Cell Death. Cell. 2019 Jul 11;178(2):302-315.e23. doi: 10.1016/j.cell.2019.05.035. PMID: 31299200; PMCID: PMC6693521.
38. Hou XM, Zhang XH, Wei KJ, Ji C, Dou SX, Wang WC, Li M, Wang PY. Cisplatin induces loop structures and condensation of single DNA molecules. Nucleic Acids Res. 2009 Apr;37(5):1400-10. doi: 10.1093/nar/gkn933. Epub 2009 Jan 7. PMID: 19129234; PMCID: PMC2655688.
39. Kasparkova J, Thibault T, Kostrhunova H, Stepankova J, Vojtiskova M, Muchova T, Midoux P, Malinge JM, Brabec V. Different affinity of nuclear factor-kappa B proteins to DNA modified by antitumor cisplatin and its clinically ineffective trans isomer. FEBS J. 2014 Mar;281(5):1393-408. doi: 10.1111/febs.12711. Epub 2014 Jan 23. PMID: 24418212.

Figures

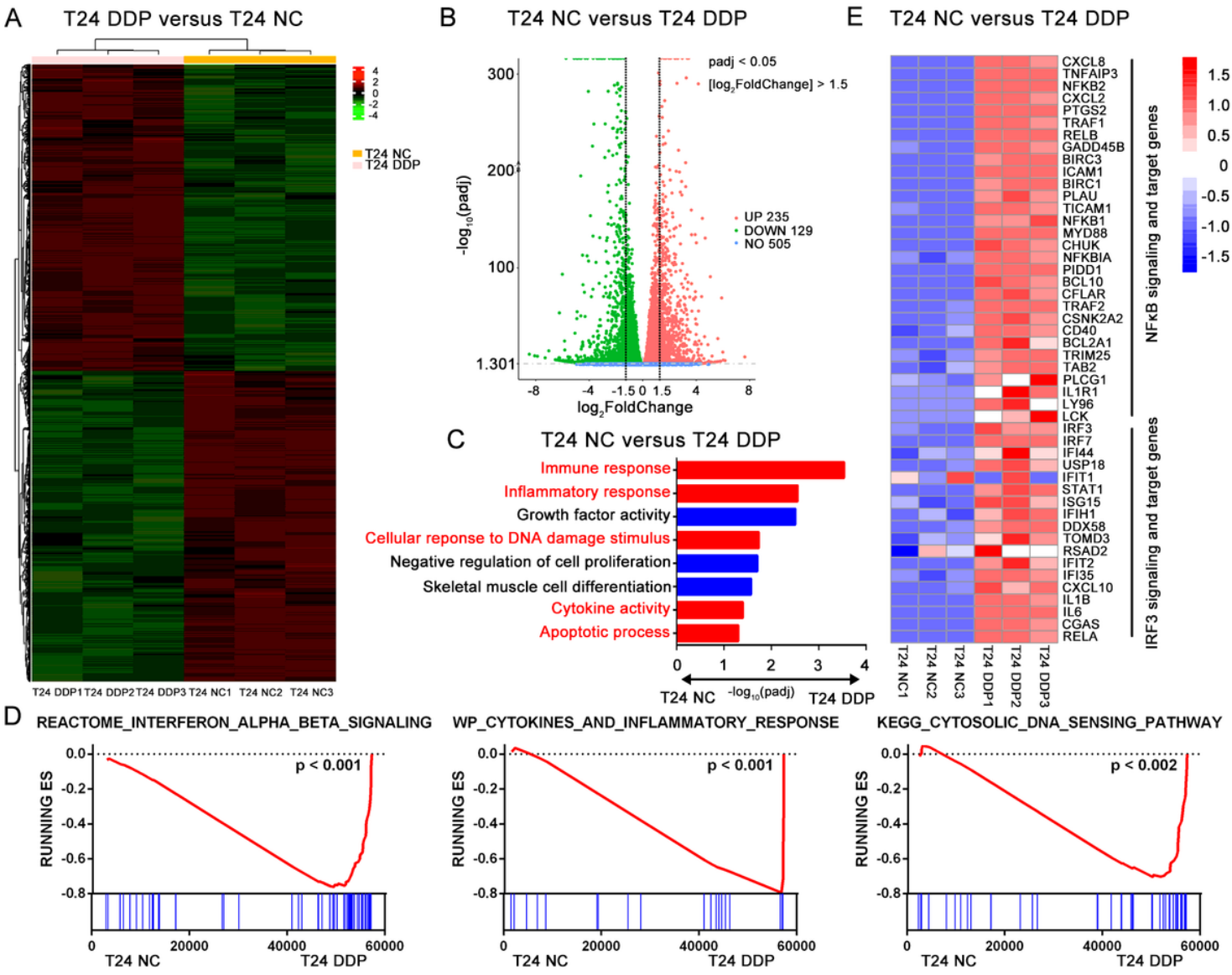

Figure 1

Cisplatin induces specific immune effects in bladder cancer cell line. T24 cell lines were treated with 2 μg/ml cisplatin (T24 DDP group) or PBS (T24 PBS group) for 24 h at standard condition. (A) The different genes expression panels between T24 DDP group and T24 PBS group were showed in heatmap. (B) Gene expression levels were quantified as Fragments Per Kilobase Million (FPKM) and then Log2–transformed as A value. The significant different expression genes were identified as absolute fold change of A value > 1.5 and Padj (adjust P) value <0.05 between two groups. Finally, the volcano map showed 235 up genes and 129 down genes with significant difference. (C) Go pathways with Padj value < 0.05 were showed here between T24 DDP group and T24 PBS group. (D) Gene set enrichment analysis (GSEA) in: Interferon α, β signaling ($P < 0.001$), cytokines and inflammatory response ($P < 0.001$) and cytosolic DNA sensing pathway ($P < 0.002$). (E) Relative transcription levels of genes expression involved in IRF3 and NF-κB signal pathway or targeting genes in T24 DDP group and T24 PBS group. Gene expression were normalized by R software from -1.5 to 1.5 (Low to high, blue to red).

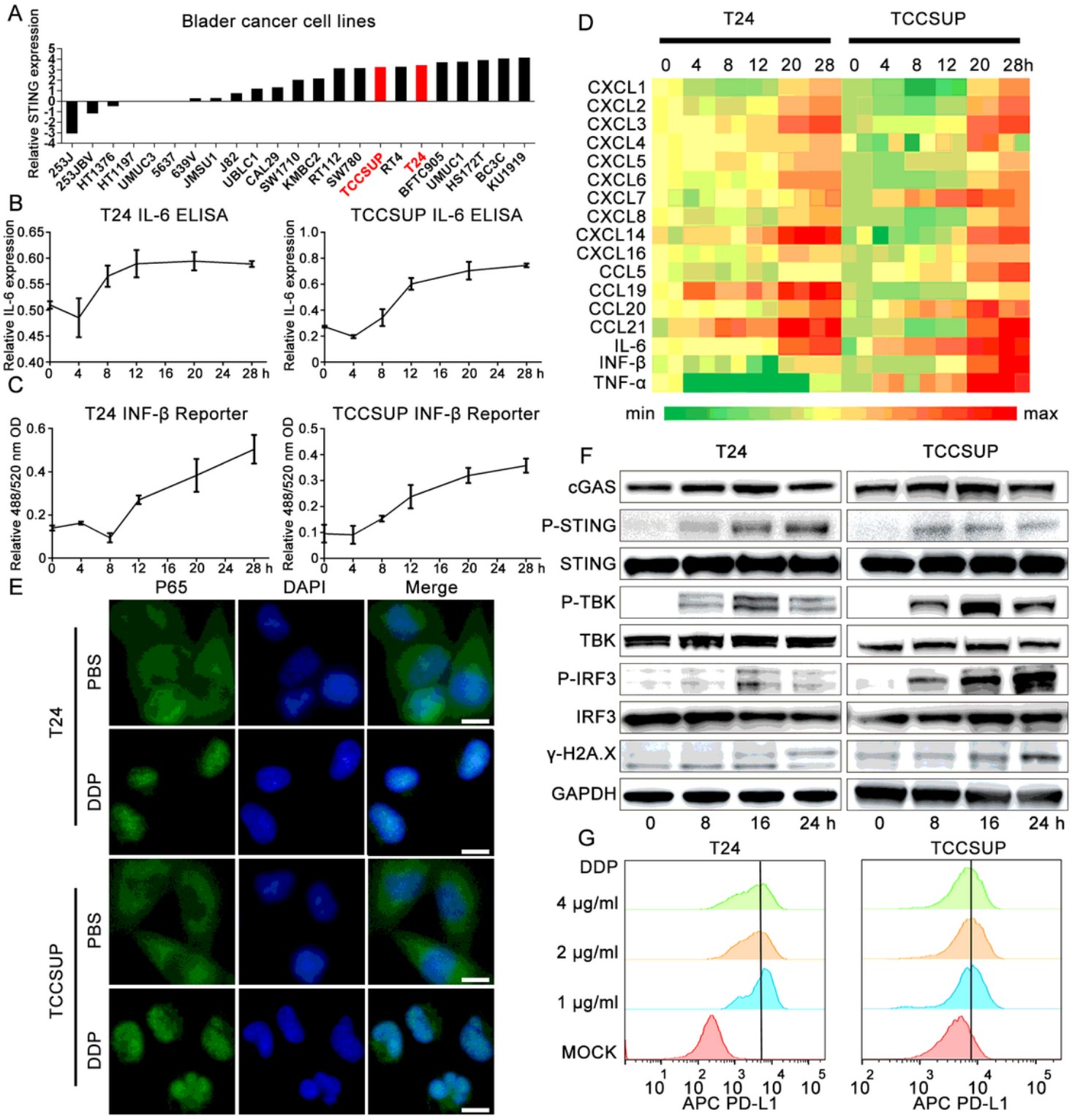

Figure 2

The immune effect of cisplatin in bladder cancer is related to the activation of cGAS-STING pathway. (A) Basic transcription levels of STING in bladder cancer cell line on CCLE database. (B-D) T24 and TCCSUP cell lines were treated with 2 μg/ml cisplatin for 0 h (control group), 4 h, 8 h, 12 h, 20 h, 28 h at standard condition, respectively. (B) ELISA analysis of IL-6 secretion in supernatants in cisplatin treated T24 and TCCSUP cell lines and corresponding control groups for different time points. (C) IFN Bio-assay in

cisplatin treated T24 and TCCSUP cell lines and corresponding control groups for different time points. (D) qRT-PCR analysis of cytokines and chemokines expression in cisplatin treated T24 and TCCSUP cell lines and corresponding control groups for different time points. Shown are genes induced at least 2 repeats. (E) Immunofluorescence assay showed subcellular distribution of p65 in T24 and TCCSUP cell lines treated with 2 μg/ml cisplatin or PBS for 24 h. Scale bar represent 5 μm. (F) Western blotting results of key proteins involved in cGAS-STING pathway in T24 and TCCSUP cell lines treated with 2 μg/ml cisplatin for 0 h, 4 h, 8 h, 12 h, 24 h, respectively. GAPDH was used as control protein. (F) Cell surface PD-L1 levels in T24 and TCCSUP cell lines treated with 1, 2 or 4 μg/ml cisplatin or PBS for 24 h.

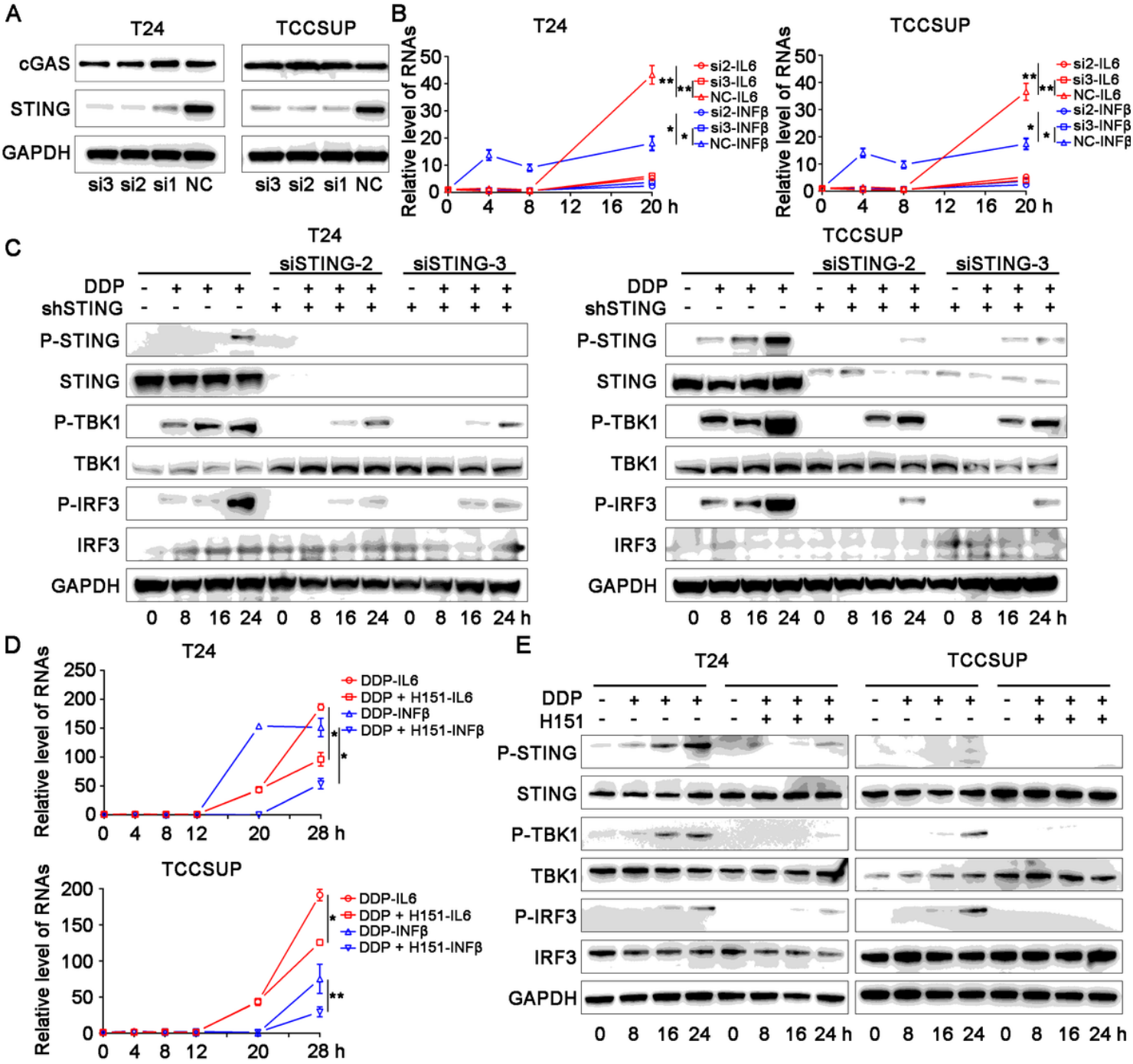

Figure 3

STING targeting siRNAs and STING specific inhibitor H151 significantly reversed cisplatin related immune effects. (A) Knockdown efficiency validation of STING in T24 and TCCSUP cell lines. GAPDH was used as control protein. (B) T24 and TCCSUP cell lines were treated with non-targeting (Scramble, Scr) or two STING-targeting siRNA (si2 and si3) for 48 h before treatment with 2 μg/ml cisplatin for 0 h, 4 h, 8 h, 12 h, 16 h, 20 h, respectively. IFN-β mRNA and IL-6 mRNA were then analyzed by qRT-PCR. (C) Western blotting results of key proteins involved in cGAS-STING pathway in T24 and TCCSUP cell lines treated with non-targeting (Scramble, Scr) or two STING-targeting siRNA (si2 and si3) for 48 h before treatment with 2 μg/ml cisplatin for 0 h, 8 h, 16 h, 24 h, respectively. GAPDH was used as control protein. (D) T24 and TCCSUP cell lines were co-treated with DMSO or H151 and 2 μg/ml cisplatin for 0 h, 4 h, 8 h, 12 h, 20 h, 28 h, respectively. IFN-β mRNA and IL-6 mRNA were then analyzed by qRT-PCR. (E) Western blotting results of key proteins involved in cGAS-STING pathway T24 and TCCSUP cell lines co-treated with DMSO or H151 and 2 μg/ml cisplatin for 0 h, 8 h, 16 h, 24 h, respectively. GAPDH was used as control protein.

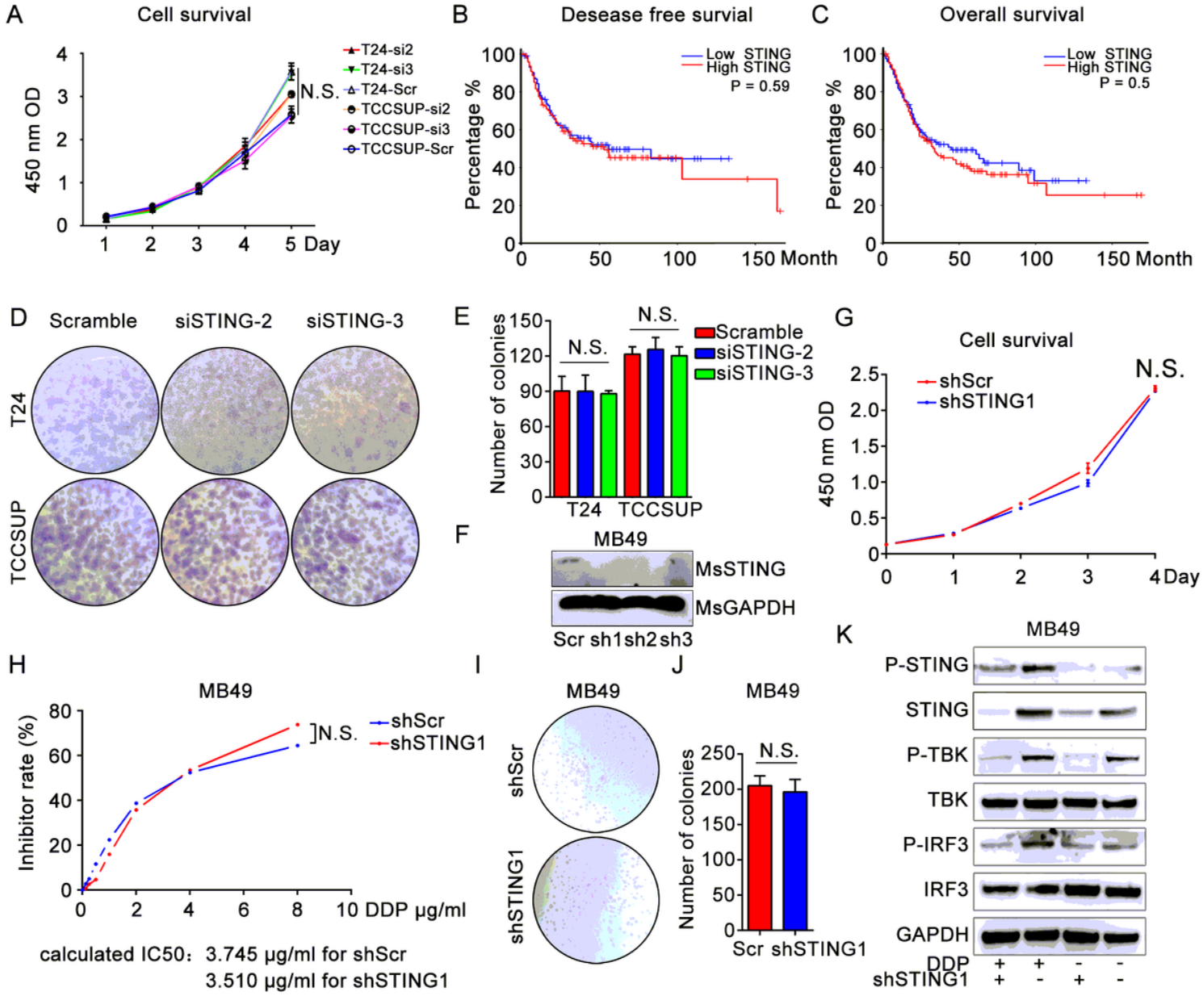

Figure 4

Modulation of STING did not affect the proliferation of bladder cancer in vitro. (A) T24 and TCCSUP cell lines were treated with non-targeting (Scramble, Scr) or two STING-targeting siRNA (si2 and si3) for 48 h before adding 1640 medium containing 10% CCK-8 regent. The 450 mm OD of each groups were measure at day 1, 2, 3, 4, 5. (B, C) Kaplan-Meier analysis of (B) overall survival rates and (C) disease-free survival rates stratified by low STING expression (n = 201) and high STING expression (n = 201) from The Cancer Genome Atlas (TCGA) database. The median was used as the dividing line, and STING upregulation showed none significantly associated with overall and disease-free survival rates. DDP, cisplatin. (D, E) Clonal formation assay of T24 and TCCSUP cell lines treated with non-targeting (Scramble, Scr) or two STING-targeting siRNA (si2 and si3) for 48 h. (F) Knockdown efficiency validation of shSTING lentivirus in MB49 cell lines. GAPDH was used as control protein. (G) MB49 cell lines were treated with non-targeting (Scramble, Scr) lentivirus or STING-targeting lentivirus for 48 h before adding 1640 medium containing 10% CCK-8 regent. The 450 mm OD of each groups were measure at day 0, 1, 2, 3, 4. (H) Calculated cisplatin IC50 of MB49 cell lines treated with non-targeting (Scramble, Scr) lentivirus or STING-targeting lentivirus for 48 h. (I, J) Clonal formation assay of MB49 cell lines treated with non-targeting (Scramble, Scr) lentivirus or STING-targeting lentivirus for 48 h. (K) Western blotting results of key proteins involved in cGAS-STING pathway in MB49 cell lines treated with 2 μg/ml cisplatin or PBS for 24 h combined with or without STING-targeting treatment. GAPDH was used as the control protein. DDP, cisplatin. N.S., $P > 0.05$.

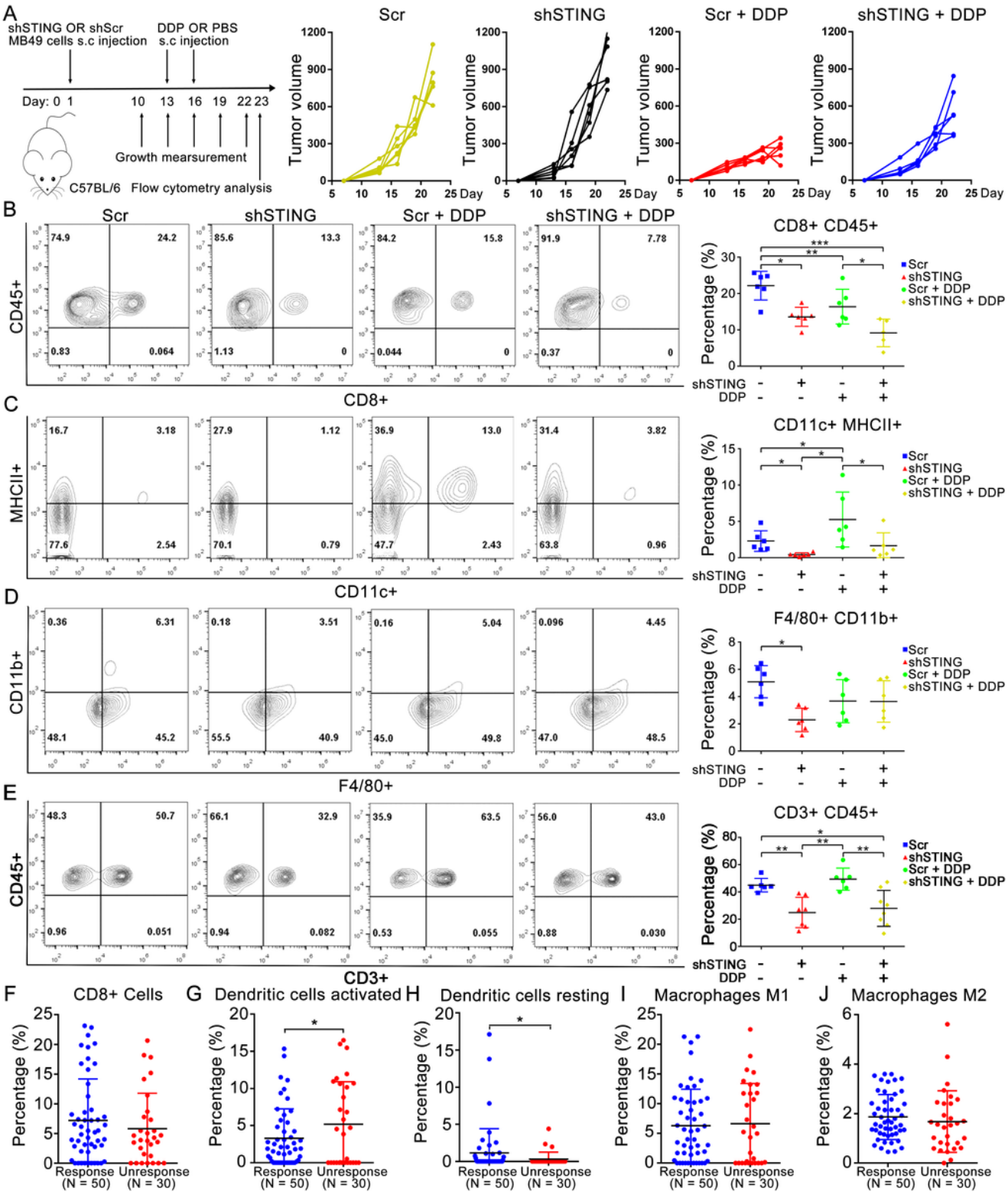

Figure 5

Activation of cGAS-STING suppressed bladder cancer in cisplatin-treated C57 mice. (A) Establish of bladder cancer transplantation models in C57 mice, left. Tumor volumes of different groups, right. (B-E) Infiltration percentages of (B) CD8+, CD45+ T cells, (C) CD11b+, MHC□+ DCs, (D) F4 / 80+, CD11c+ Macrophage, (E) CD3+, CD45+ cells in MB49 xenograft transplantation tumors. (F-J) CYBERSORT predicted infiltration percentages of CD8+ T cells (F), DCs activated cells (G), DCs resting cells (H),

Macrophages M1 cells (l), and Macrophages M2 cells in response group (n = 50, CR or PR) was significantly higher than non-response group (n = 30, PD or SD) after cisplatin based chemotherapy. *P < 0.05, **P < 0.01, ***P < 0.001. DDP, cisplatin.

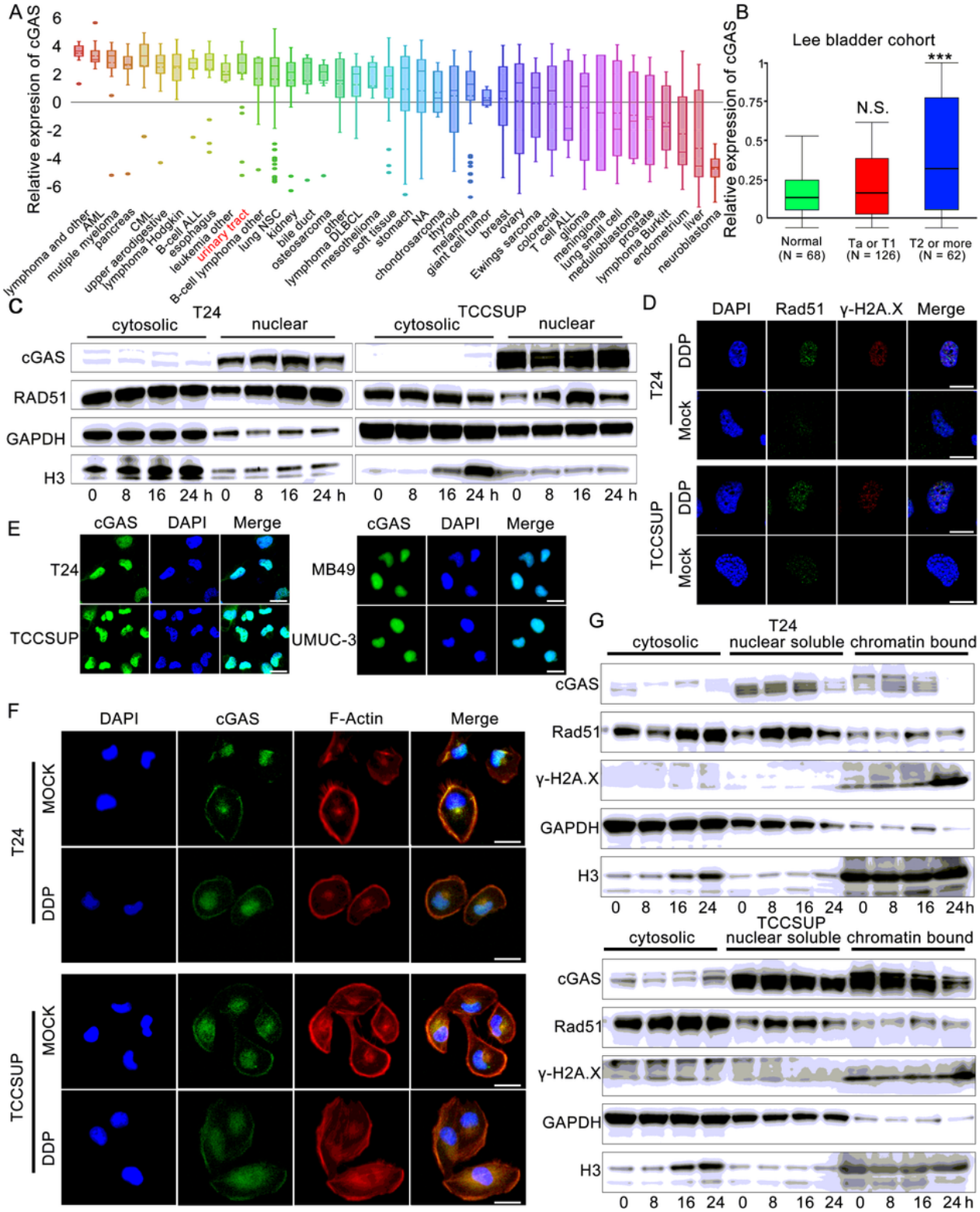

Figure 6

Cisplatin induced dsDNA and the releasing of chromatin bound cGAS may function as an important role in enhancing STING signal. (A) Basic transcription levels of cGAS in bladder cancer cell line on CCLE

database. (B) Relative transcriptional expression of cGAS in different T stages (Normal N = 68, Ta or T1 N = 126 and T2 or more N = 62) in Lee bladder cohort. (C) Western blotting of subcellular distribution of cGAS, Rad51 GAPDH and Histone H3 proteins. GAPDH was used as cytosolic control protein, and histone H3 was used as nuclear control proteins. T24 and TCCSUP cell treated with 2 μg/ml cisplatin or PBS at 0 h, 8 h, 16 h, 24 h time points. (D) Immunofluorescence of expression and distribution of Rad51 and γ-H2A.X proteins in T24 and TCCSUP cell lines treated with μg/ml cisplatin or PBS for 24 h. DDP, cisplatin. Scale bar represent 10 μm. (E) Immunofluorescence of cGAS subcellular distribution of T24, TCCSUP, MB49 and UMUC-3 cell lines. Scale bar represent 5 μm. (F) Immunofluorescence of cGAS subcellular distribution of T24 and TCCSUP cell lines treated with 2 μg/ml cisplatin or PBS. Scale bar represent 5 μm. (G) Western blotting of subcellular distribution of cGAS, Rad51, γ-H2A.X, GAPDH and Histone H3 proteins. GAPDH was used as cytosolic and nuclear soluble control protein, and Histone H3 was used as chromatin bound control proteins. T24 and TCCSUP cells were treated with 2 μg/ml cisplatin or PBS at 0 h, 8 h, 16 h, 24 h time points. DDP, cisplatin, N.S., $P > 0.05$, ***$P < 0.001$

Supplementary Files

This is a list of supplementary files associated with this preprint. Click to download.

- FigureS1.tif
- FigureS2.tif
- FigureS3.tif
- TableS1.docx
- Figure7.png